International Journal of Engineering Research & Technology (IJERT)
ISSN: 2278-0181
Vol. 5 Issue 04, April-2016

Augmentation of Classical and Adaptive Control for Second Generation Launch Vehicles

Smrithi U S
Asst. Professor, EEE Department
Ace College of Engineering
Thiruvananthapuram, India

Dr. Brinda V
Head, Control Design Division
Vikram Sarabhai Space Centre
Thiruvananthapuram, India

***Abstract*— Classical control technique is used for attitude control of launch vehicles worldwide, because of its established history of success. Usual method is to model launch vehicle dynamics by linear techniques to achieve adequate stability and tracking performance. Common type of feedback control system for launch vehicles is the Proportional-Integral (PI) controller with appropriate filters to stabilize the lateral bending modes and slosh modes and also ensure sufficient robustness margins for rigid body. This paper presents a Classical Adaptive Augmentation Control (AAC) Algorithm for forward loop gain augmentation in real time, to cater to large dispersion in vehicle parameters beyond the capability of classical control system. The idea is to provide augmentation to a classical control designed autopilot when performance enhancement is required to tackle off-nominal conditions arising out of modeling errors and large dispersion in estimated vehicle parameters (thrust, inertia, slosh, aerodynamics, lateral bending modes). There is high chance that such large dispersion can arise during initial design of a new generation launch vehicle before actual flight. Finally, simulation results for several credible launch vehicle failure scenarios show that the adaptive controller consistently and predictably improves performance and robustness, and achieves stability during extreme off-nominal situations.**

Keywords—Adaptive Controlt; Augmentation; Parameter Uncertainty; Gain Schedulling; Robustness

I. INTRODUCTION

As Launch Vehicles pace up along with the development of new technologies, the core targets of new designs are to enhance payload capability (performance), reliability, and safety at decreasing cost. As computational capability has become advanced, control algorithms play a major role towards achieving this aim. Global control algorithm used in current generation launch vehicles is the Proportional Integral (PI) control with gain scheduling. Although much advancement have taken place over the last few years, PI with gain scheduling control remains dominant due to its strong heritage. Generally, attitude control problem is considerate of the short period dynamics of the vehicle, where the basic aim is to achieve adequate stability and reasonably rapid response to input guidance commands, with average passivity to external disturbances. Launch vehicles are often aerodynamically highly unstable. Despite that, launch vehicle dynamics are readily modeled in literature using linear techniques to arrive at an autopilot configuration that meets the design requirements. For the flight control systems design, the consolidations of Blakelock[1], Greensite[2], and Garner[5] are quite all-inclusive.

Major design problems exist because a launch vehicle is aerodynamically unstable, highly flexible and additional problems due to sloshing of liquid propellants and the inertia effects of engines. These problems are seriously aggravated for certain advanced launch vehicle configurations. Under such a scenario, classical control methods may not be fully effective in meeting the robustness margins for very large dispersions in vehicle parameters mainly because they are not known with sufficient precision before flight. Because a failure of any one of components could mean loss of the vehicle, an extensive ground testing and evaluation program is necessary to provide the maximum confidence for successful flight. This has led to the focus in adaptive control technique.

Greatest benefit of adaptive control that can be exploited is the fact that they don't require a deductive knowledge of the launch vehicle parameters with great accuracy. A survey of Adaptive Control Systems by Astrom, et al., in [6] clarifies the immense potential of the approach. In order to fully extract the benefits of adaptive control for a particular application, the adaptive control system must be designed with knowledge of the complete system to which it is to be applied [7], [8], [9]. This includes general features of the aerospace vehicle, such as control-structure interaction, sloshing of propellants, performance of sensors, and actuator dynamics. Out of the many adaptive control schemes, the direct Model Reference Adaptive Control (MRAC) shows robustness to uncertainties with sometimes improved and more predictable performance, [10], [11], [12].

An algorithm that relies on model reference-driven gain adaptation supplemented by spectral damping is demonstrated by Jeb S Orr, et al., in [13]. The focus is on adaptive control developments that are specifically tuned for application to launch vehicles which maintains consistency with classical control system design.

This paper presents implementation and validation of a classical Adaptive Augmentation Control (AAC) algorithm for a typical 2^{nd} generation launch vehicle, for performance enhancement in the event of large deviations in estimated vehicle parameters. AAC provides minimum augmentation when vehicle is under the control of classical controller within an expected range of parameter variations and environment uncertainty. However, if classical controller is unable to render sufficient performance due to parameter variation, external disturbances etc., the adaptive controller modifies the output of the classical feedback control law so as to maintain stability and minimize performance loss to the maximum possible extent. The analysis reveals that AAC can be implemented on board safely without affecting the

International Journal of Engineering Research & Technology (IJERT)
ISSN: 2278-0181
Vol. 5 Issue 04, April-2016

nominal and off nominal performances within bounds and at the same time ensure best results for unpredicted severe dispersions thus avoiding vehicle failure possibilities. By incorporating the AAC technique, the practice of assessing flight control stability using classical gain and phase margins is not affected under justifiable assumptions.

The paper is organized in 6 sections. After a brief introduction of the topic in section I, section II describes the mathematical model of launch vehicle in pitch plane. Classical controller design is explained in section III. Section IV deals with the classical adaptive augmentation (AAC) scheme and its validation is presented in section V. Finally, the paper is concluded in section VI.

II. LAUNCH VEHICLE MODELING

A. *Equations of short period dynamics*

The primary objective of Launch Vehicle Attitude Control System is to orient the vehicle along the required trajectory in the presence of external disturbances. First step towards this is to model the vehicle attitude dynamics taking into account aerodynamics, control actuator dynamics, vehicle bending, propellant sloshing, variation in center of gravity (cg) and moment of inertia etc. as the time progresses. This leads to a time variant system. Using time slice approach a short period model is evolved [2] which can be assumed time invariant for a small duration, so that linear time invariant control system principles can be used. Further it is assumed to be decoupled in pitch/yaw/roll and planar analysis is carried out. Referring to [2],[3], the equations of short period dynamics can be represented as

1) Rigid body

Consider the geometry of vehicle in pitch plane represented in Fig 1.

$$\frac{\ddot{z}}{U_0} = \frac{\sum F_z}{m_0 U_0} + \dot{\theta} \tag{1}$$

$$I_{yy}\ddot{\theta} = \sum M_y \tag{2}$$

Considering the forces and moments acting on the launch vehicle due to engine inertia, aerodynamics, elasticity, slosh and actuator effects, effective force and moment equations may be represented as

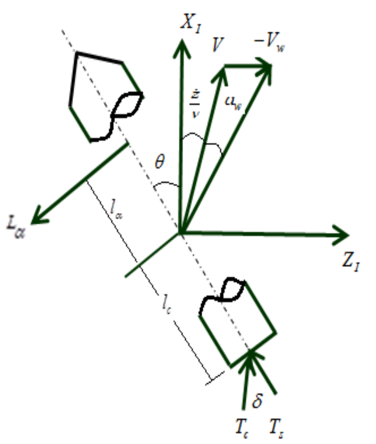

Fig. 1. Geometry of vehicle in pitch plane

<u>Force Equation</u>

$$\sum F_z = T_c\delta - T_T \sum q^{(i)}\sigma^{(i)}\left(l_T\right) - \frac{1}{2}\rho U_0^{\,2} A[C_n l_\alpha \alpha] + \sum_i m_{pi}\dot{U}_0\tau_{pi} + m_r[l_r\ddot{\delta} + \left(l_c - l_r\right)\ddot{\theta} - \dot{w} + \dot{U}_0\theta] - \sum_i\left[\psi^{(i)}\left(l_T\right) + l_r\sigma^{(i)}\left(l_T\right)\right]m_r\ddot{q}^{(i)}. \tag{3}$$

<u>Moment Equation</u>

$$\sum M_y = l_c[T_c\delta - T_T\sum q^{(i)}\sigma^{(i)}(l_T)] - T_T\sum q^{(i)}\psi^{(i)}(l_T) + \frac{1}{2}\rho U_0^{\,2}A\,[C_n l_\alpha\alpha] + \sum_i m_{pi} l_{p_i}\dot{U}_0\tau_{pi} + [I_r + m_r l_r l_c]\ddot{\delta} + m_r l_r \dot{U}_0\delta - [I_r - m_r l_c^{\,2}]\ddot{\theta} - m_r[l_r + l_c]\dot{w} + m_r l_c\dot{U}_0\theta - m_r l_c\dot{U}_0\sum\sigma^{(i)}(l_T)q^{(i)} - \sum_i\left[m_r(l_r + l_c)\psi^{(i)}(l_T) + (I_r + m_r l_r l_c)\sigma^{(i)}(l_T)\right]\ddot{q}^{(i)} \tag{4}$$

2) Slosh mode

Fuel-slosh can be a severe issue in space vehicle stability and control. Dynamic effects of a sloshing liquid can be nearly approximated by replacing the liquid mass with a rigid mass and a harmonic oscillator like pendulum. Using the pendulum parameters like mass, length, hinge point location etc., the equation of motion of the ith pendulum can be represented as

$$\ddot{\tau}_{pi} + w_{pi}^{\,2}\tau_{pi} = \frac{1}{L_{pi}}[\dot{U}_0\theta - \dot{w} + \ddot{\theta}(l_{pi} - L_{pi}) + \sum\ddot{q}^{(i)}\psi^{(i)}l_{pi}] \tag{5}$$

3) Bending mode

The elastic deflection at any point along the vehicle [3] is given by

$$\xi(l,t) = \sum_i\left(q^{(i)}\right)^2(t)\psi^{(i)}(l) \tag{6}$$

where $\psi^{(i)}(l)$ denotes the normalized mode shape of the ith mode in the pitch plane. $q^{(i)}(t)$ is the generalized co-ordinate due to elasticity for the ith mode in the pitch plane. It satisfies the equation

$$\ddot{q}(t) + 2\zeta_i w_i\dot{q}^{(i)} + w_i^{\,2}q^{(i)} = -\frac{Q^{(i)}}{M^{(i)}} \tag{7}$$

where $Q^{(i)}$ and $M^{(i)}$ are the generalized force and mass respectively and are given by

$$Q^{(i)} = \int_0^L f_p(l,t)\psi^{(i)}(l)dl \tag{8}$$

$$M^{(i)} = \int_0^L m(l)\left[\psi^{(i)}\right]^2 dl \tag{9}$$

4) Actuator

The second order actuator dynamics may be represented as

$$\ddot{\delta}_A = -w_A^{\,2}\delta_A + w_A^{\,2}\delta_C - 2\zeta_A w_A\dot{\delta}_A \tag{10}$$

5) Nozzle

The second order nozzle dynamics may be represented as

International Journal of Engineering Research & Technology (IJERT)
ISSN: 2278-0181
Vol. 5 Issue 04, April-2016

$$\ddot{\delta}_N = \frac{[I_r + m_r l_r l_c]}{I_r}\ddot{\theta} - \frac{m_r l_r}{I_r}\ddot{z} + w_N^2(\delta_A - \delta_N) - 2\zeta_N w_N \dot{\delta}_N \quad (11)$$

B. State Space Representation

The complete plant dynamics represented by equations (3) to (11) may be expressed in the state space form given by

$$K\dot{x} = Ax + Bu \quad (12)$$

$$\dot{x} = K^{-1}Ax + K^{-1}Bu$$
$$y = Cx + Du \quad (13)$$

where 15 states are chosen considering rigid body mode, 3 bending modes, 1 slosh mode, actuator and nozzle dynamics given by

$$x = [\theta;\dot{\theta};\dot{z};q^{(1)};\dot{q}^{(1)};q^{(2)};\dot{q}^{(2)};q^{(3)};\dot{q}^{(3)};\tau;\dot{\tau};\delta_N;\dot{\delta}_N;\delta_A;\dot{\delta}_A] \quad (14)$$

The control input is the deflection angle:

$$u = [\delta_c] \quad (15)$$

The output:

$$y = \begin{bmatrix} \theta & \dot{\theta}_{ag} & \dot{\theta}_{rg} \end{bmatrix}^T \quad (16)$$

where θ is the pitch angle, $\dot{\theta}_{ag}$ and $\dot{\theta}_{rg}$ represent the pitch rate sensed by angle and rate gyros respectively.

The launch vehicle model used for analysis consists of two large solid boosters strapped into a liquid core. Initial analysis is done at the atmospheric flight stage at a particular instant where aerodynamic forces are significant. Using the vehicle parameters and by considering the effect of two nozzles at the solid boosting phase, the governing equations are modified and rearranged to get required state space matrices.

C. Simplified System Modeling

For the purpose of investigating the general features of a highly simplified version of the control system, equations (3)-(11) may be reduced to any simplified degree. Ignoring the effects of bending, sloshing and effects due to actuator dynamics, the plant dynamics may be expressed in the transfer function form as

$$\frac{\theta(s)}{\delta_p(s)} = \frac{\mu_c}{s^2 - \mu_\alpha} \quad (17)$$

where the control moment coefficient, $\mu_c = \dfrac{T_c l_c}{I_{yy}}$ (18)

the aerodynamic moment coefficient, $\mu_\alpha = \dfrac{L_\alpha l_\alpha}{I_{yy}}$ (19)

III. CLASSICAL CONTROL DESIGN METHOD

Autopilot design for a launch vehicle is carried out in a conventional way using the classical control techniques [4]. This is well established method when performance criteria for control system are expressed in terms of undamped natural frequency, damping factor, steady state errors gain margins, phase margins, etc. The method of pole placement is used for control system design of a conventional launch vehicle. Here the design/response specifications can be transformed into desired locations of dominant closed loop poles. Using the model developed, the control system gains are selected so as to place the closed loop poles in the above locations. The gains are obtained as function of vehicle parameters and closed loop poles.

Control system design is carried out in two phases, first for a simplified model without slosh and flexibility. Gains are selected for good tracking, rapid response and good damping ensuring the system stability as the time progresses. In the next step a suitable compensator is designed to stabilize the bending modes and sloshing modes as well as improving the rigid body margins in presence of higher order dynamics.

A. Simplified Autopilot Architecture

1) Block diagram of simplified Autopilot

The block diagram of launch vehicle rigid body model with a simplified autopilot is shown in fig.2. K_A is the forward loop gain and K_R, the rate gyro gain.

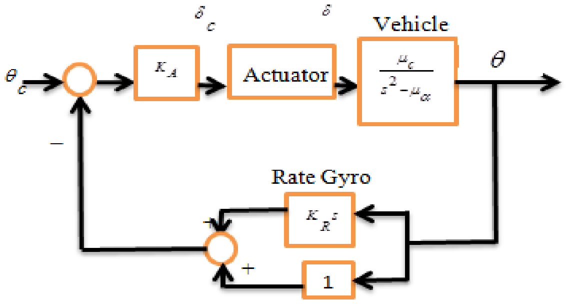

Fig. 2. Block diagram of Simplified Autopilot

The closed loop transfer function of the simplified rigid body model is given by

$$\frac{\theta(s)}{\theta_c(s)} = \frac{G(s)}{1+G(s)H(s)} = \frac{K_A\mu_c}{s^2 + K_A\mu_c K_R s + (K_A\mu_c - \mu_\alpha)} \quad (20)$$

2) Design of simplified Autopilot

In the transfer function given by equation (20), the values of K_A, the forward loop gain and K_R, the rate gyro gain at a particular time instant have to be determined. The characteristic equation of the simple rigid body model with simplified autopilot is given by

$$s^2 + K_A\mu_c K_R s + (K_A\mu_c - \mu_\alpha) = 0 \quad (21)$$

Equation (21) can be compared with the characteristic equation of a typical second order system

$$s^2 + 2\zeta\omega_n s + \omega_n^2 = 0 \quad (22)$$

where ω_n and ζ represent the undamped natural frequency and damping factor respectively

Comparing (21) & (22), we get

International Journal of Engineering Research & Technology (IJERT)
ISSN: 2278-0181
Vol. 5 Issue 04, April-2016

$$K_A = \frac{\omega_n^2 + \mu_\alpha}{\mu_c} \tag{23}$$

$$K_R = \frac{2\zeta\omega_n}{\omega_n^2 + \mu_\alpha} \tag{24}$$

From (18) and (19), we have

$$\mu_c = 5.35 \text{ and } \mu_\alpha = 1.8 \tag{25}$$

For a desirable rigid body natural frequency ω_n =3 rad/sec and damping factor, ζ = 0.75, and substituting the same in (23) & (24) gives

$$K_A = 2 \text{ and } K_R = 0.44 \tag{26}$$

An increase in value of K_A provides best performance and decrease the steady state error associated, but it affects the stability features. Hence Proportional Integral Control strategy may be introduced to maintain required performance capability without losing stability.

B. PI Controller Architecture

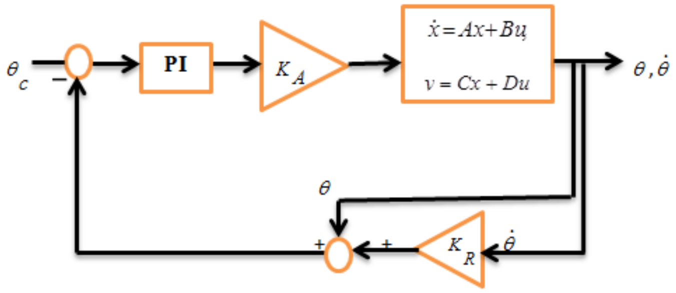

Fig.3. Classical Controller Architecture

The block diagram/architecture of PI controlled system is shown in fig. 3. Design of classical controllers like P/PI/PID controllers can be done using the classical root locus technique based on time domain approach where a controller can be designed in cascade with the system to have a pair of dominant closed loop poles which satisfy specified time domain specifications ω_n and ζ. Here, without changing the position of already placed dominant poles significantly, damping factor is slightly changed so as to eliminate steady state error.

If $G(s_d = D\angle\beta) = A_d\angle\phi_d$ is the open loop transfer function of the system and $G_c(s_d = D\angle\beta)$ is the transfer function of PID controller with respect to the dominant pair pole (s_d) location, satisfying the magnitude condition for dominant pole pair to be on the root locus, the proportional, integral and derivative gains of a PID controller in general can be derived as

$$K_d = \frac{\sin\phi_d}{DA_d \sin\beta} + \frac{K_i}{D^2} \tag{27}$$

$$K_p = \frac{-\sin(\beta + \phi_d)}{A_d \sin\beta} - \frac{2K_i \cos\beta}{D} \tag{28}$$

where K_i is determined such that specified error constant is met. For designing PI controller, the value of K_d is assumed to be zero in (27). Hence the design equations are

$$K_i = \frac{-D\sin\phi_d}{A_d \sin\beta}; \; K_p = \frac{-\sin(\beta + \phi_d)}{A_d \sin\beta} - \frac{2K_i \cos\beta}{D} \tag{29}$$

The dominant pole for ζ =0.75 and ω_n =3 rad/s,

$$s_d = D\angle\beta = 2.99\angle 138.6^\circ \tag{30}$$

Referring to Fig. 2.,

$$G(s)H(s) = \frac{K_A\mu_c(1 + K_R s)}{s^2 - \mu_\alpha} \tag{31}$$

With respect to the dominant pole location,

$$G(s)H(s)\Big|_{s_d} = A_d\angle\phi_d = 1.043\angle 184.03^\circ \tag{32}$$

Integral constant, K_i and proportional constant K_p are obtained from equation (29) as

$$K_i = 0.3 \quad K_p \cong 1 \tag{33}$$

The controller transfer function becomes

$$G_c(s) = K_p + \frac{K_i}{s} = (1 + \frac{0.3}{s}) \tag{34}$$

The designed values are applied on simplified system model as well as the complete plant model with a suitable compensator designed (a lag filter) for phase stabilization and tuned until a stable system with satisfactory performance is achieved.

IV. CLASSICAL ADAPTIVE AUGMENTATION CONTROL ALGORITHM DESIGN

A. Control Architecture

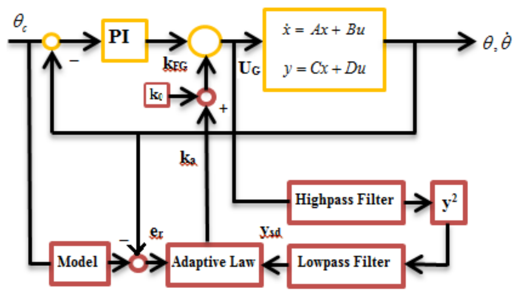

Fig.4. Classical Adaptive Augmentation Control

Fig. 4 represent the block diagram of augmented Adaptive Control. By working as an augmenting controller rather than the primary method of accommodating the changing flight scenarios, the design preserves the strength of classical controller during nominal situations

Published by :
http://www.ijert.org

International Journal of Engineering Research & Technology (IJERT)
ISSN: 2278-0181
Vol. 5 Issue 04, April-2016

B. Zones Of Adaptation

The three main zones where adaptation is expected to work are the following

- Respond to tracking error
- Respond to undesirable control-structure interaction
- Return to baseline control design during nominal cases

C. Adaptation Law [14]

A multiplicative first-order adaptation law is used,

$$\dot{k}_a = \left(\frac{k_{max} - k_a}{k_{max}}\right) a e_r^{\ 2} - b k_a y_{sd} - c\left(k_{FG} - 1\right) \qquad (35)$$

where e_r is the model error, y_{sd} is the damper signal and *a*, *b*, *c* represents the error gain, damper gain and nominal gain respectively. The error term responds to tracking error, the damper term during control-structure interaction and the nominal term for automatic re-convergence to PI controller, when adaptation is not needed. An upper and lower bound to adaptation is provided given by k_{max} and k_0. For at least 6 dB robustness gain margin which corresponds to a magnitude of 2, k_{max} is chosen as 1.5 and k_0 is chosen as 0.5.

The output of the adaptive law is the adaptive gain k_a, which is used to adjust the output of the PI controller. The adaptive gain k_a is used to calculate a total forward loop gain given by

$$k_{FG} = k_0 + k_a \qquad (36)$$

1) Computation of error term, e_r

The error term is the part which increases the adaptive gain, when needed. A reference model is designed to attain the desired closed loop performance, similar to second order rigid body system that tracks the guidance commands.

$$\begin{bmatrix} \dot{\theta}_r \\ \ddot{\theta}_r \end{bmatrix} = \begin{bmatrix} 0 & 1 \\ -(\omega_r)^2 & -2\xi_r\omega_r \end{bmatrix} \begin{bmatrix} \theta_r \\ \dot{\theta}_r \end{bmatrix} + \begin{bmatrix} \omega_r^{\ 2} \\ 0 \end{bmatrix} \theta_c \qquad (37)$$

$$e_r = d\ \left(\theta_r - \theta\right) \qquad (38)$$

where *d* is the error mixing constant

2) Computation of damper signal, y_{sd}

Damper signal is a rectified signal detecting and passing undesirable high-frequency dynamics in the loop. Decay of adaptive gain is proportional to magnitude of signal.

$$y_{HP} = H_{HP}(s) U_G \qquad (39)$$

$$y_{sd} = H_{LP}(s)\left(y_{HP}\right)^2 \qquad (40)$$

y_{HP} and y_{sd} are outputs of a High pass filter and a Low pass filter being used, with transfer functions H_{HP} and H_{LP} respectively.

a) High pass filter

A high pass Chebyschev filter is used with a cut off frequency approximately twice of that of the rigid body frequency.

b) Low pass filter

A maximally flat Butterworth filter of cut off frequency approximately nearing the rigid body control frequency is chosen here. The frequency responses of High pass and Low pass filter chosen are shown in fig 5.

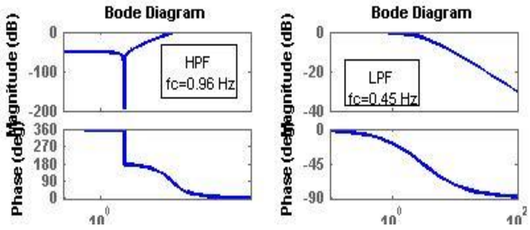

Fig.5. Frequency response of High Pass & Low Pass Filter

V. VALIDATION OF ADAPTIVE AUGMENTATION CONTROL DESIGN

In order to validate the proposed control scheme, simulations of attitude control of launch vehicle are presented. The controller is tested on the typical discretized launch vehicle model to check whether the design criteria are met.

A. Adaptive Controller Parameters

The tuned adaptation gains are given in table 1.

Table 1. Adaptive Control Parameters

Gains	Symbol	Value
Error gain	a	0.001
Damper gain	b	100
Nominal gain	c	0.2
Error mixing constant	d	25
Maximum adaptation gain	k_{max}	1.5
Minimum adaptation gain	k_0	0.5

B. Test Cases

The four credible test failure scenarios selected are

1. Minimal adaptation during nominal plant situation
2. Low thrust/high inertia (dispersed by 20%)
3. First bending mode frequency decreased by 30%
4. High thrust/Low Inertia

C. Short Period Simulations

The above mentioned test cases are tested on the modeled linear time invariant plant on short period basis initially, subjected to a steering step command, θ_c

International Journal of Engineering Research & Technology (IJERT)
ISSN: 2278-0181
Vol. 5 Issue 04, April-2016

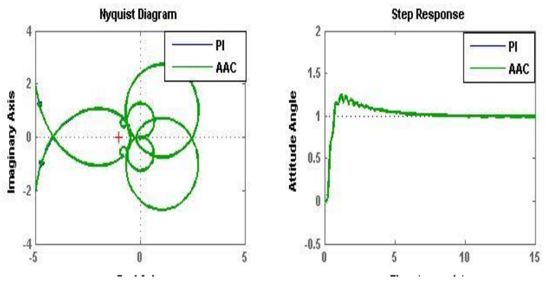

Fig.6. Nyquists & step response for case 1

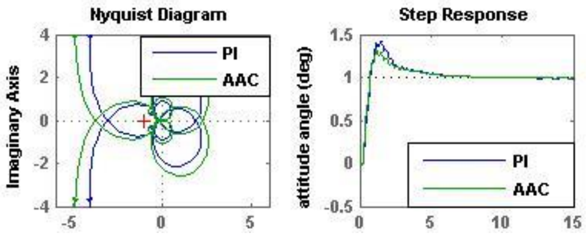

Fig.7. Nyquists & step response for case 2

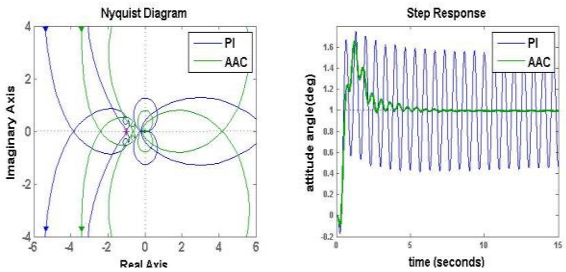

Fig.8. Nyquists & step response for case 3

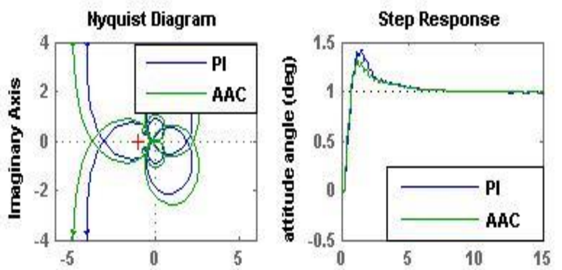

Fig.9. Nyquists & step response for case 4

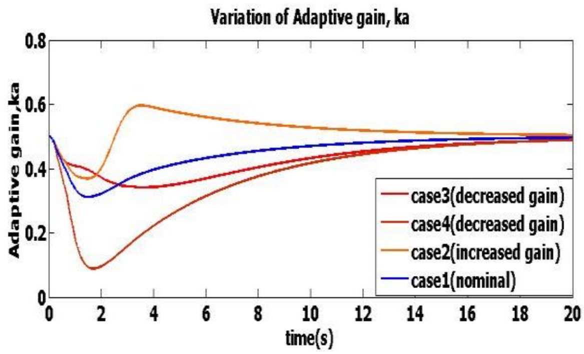

Fig.10: short period-Variation in adaptive gain for all cases

D.Planar Simulations

A long period planar simulation is carried out using vehicle data from 40 to 90 seconds with proper gain scheduling and performance of adaptation is evaluated. Here, the steering command generated by guidance is applied to the plant with time varying parameters. The plant parameters, the steering command signal and the reference model vary at each instant. Fig.11 shows the variation in scheduled gains $K_A \& K_R$

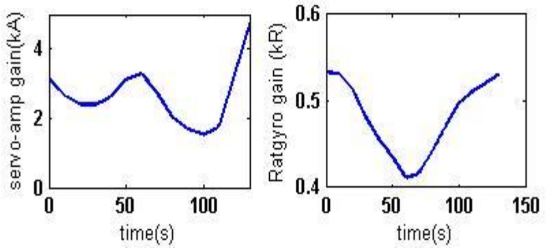

Fig. 11: Variation of scheduled gains, $K_A \& K_R$

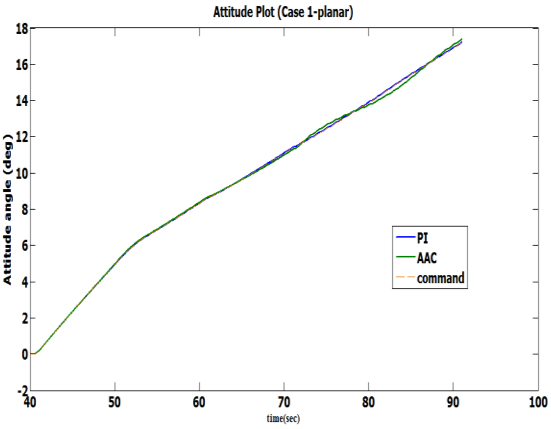

Fig. 12: Case 1: Attitude Plot

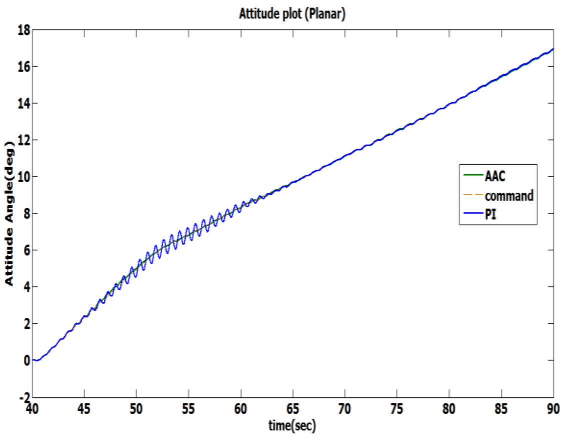

Fig. 13: Case 3: Attitude Plot

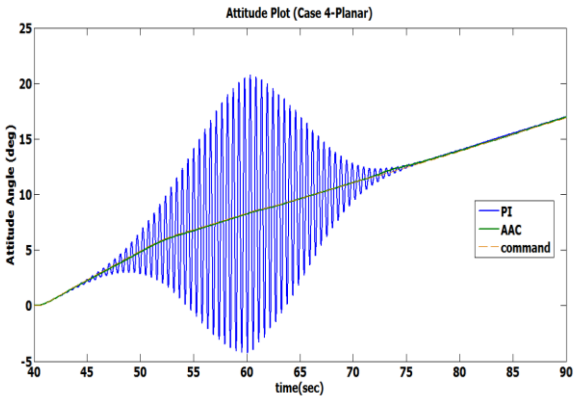

Fig. 14: Case 4: Attitude Plot

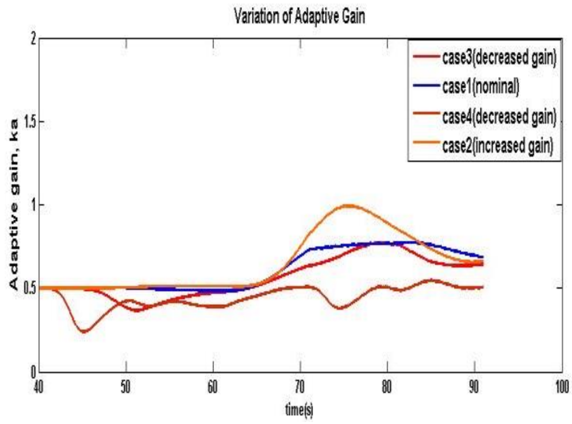

Fig.15: long period-Variation in adaptive gain for all cases

E. Analysis of Simulation Results

The simulation results for different test cases selected show that PI controller with suitable compensation works satisfactorily for nominal cases as well as for dispersions upto 20% in plant parameters. For extreme off-nominal situations tested, AAC takes the control.

In the first test case, the nominal plant is simulated. Here, the baseline controller renders reasonable performance. Thus, the contribution from AAC is minimal, as expected. From the nyquist plot shown in fig. 6, the rigid body margins obtained from short period simulation are Gain margin = 7 dB; Phase margin= 48 deg; Aero margin = 12.3 dB. For slosh mode, Phase margin= 30 deg. For first bending mode, phase margin= 47.8 deg. Step response shows an acceptable overshoot of less than 30 percent and tracking error less than 1 deg. In the planar simulation also (fig. 12), commanded attitude profile is followed satisfactorily. In Fig 10 and fig 15, k_a is maintained close to 0.5, so that total adaptive loop gain, k_{FG} is equal to 1.

In the second case, a model error is created by decreasing torque and increasing inertia by 30%. Here, PI controller deteriorates in its performance. AAC increases the adaptive gain owing to model error and improves performance and stability margins. The increase in adaptation gain is visible in both fig. 10 and fig. 15.

An unstable situation is created in third test case by introducing an unexpected extreme dispersion (30% decrease) in first bending mode frequency and mass. The PI controller degrades here to retain stability. There is a chance that the command signal gets in phase with the excited plant, increasing its amplitude further till stability is lost. AAC decreases the adaptive gain and maintains stability. Planar simulation (fig. 13) supports the short period analysis. The decrease in adaptation gain is shown in both fig. 10 and fig. 15.

In the last case, a high thrust/low inertia situation is experimented, which leads to complete loss of stability of vehicle as the PI controller gain becomes excessive. AAC decreases gain and stability is gained back. Same result is established during planar simulation as well (fig. 14).

VI. CONCLUSIONS

An adaptive augmenting strategy has been incorporated into the designed pitch axis dynamics of a typical launch vehicle to back support the classical controller (PI) designed, so as to improve performance and handle extreme off-nominal situations. Several credible test cases were selected for validating the performance supremacy of proposed controller. Simulation results show that adaptive augmentation provided sufficient performance improvement, and avoided loss of vehicle for extreme off-nominal cases. By acting as augmenting controller, classical control is maintained as the primary controller thereby preserving the strength and legacy of classical control for nominal as well as bounded dispersion cases. The method is proved to be suitable for ensuring safety of new generation launch vehicles designed for advanced missions during their initial flight testing phase. As forward work, a strict assessment of proposed scheme in a full six-degree of freedom nonlinear environment may be done to validate its use in a relevant flight environment.

REFERENCES

[1] J. Blakelock, "Stability and Control of Aircraft and Missiles", *2nd Edition* Wiley-Interscience, 1991
[2] A. Greensite, "Analysis and Design of Space Vehicle Flight Control Systems, Volume I - Short Period Dynamics," *NASA* CR-820,1967
[3] A. Greensite, "Analysis and Design of Space Vehicle Flight Control Systems, Volume XV- Elastic body equations," *NASA* CR-834,1970
[4] A. Greensite, "Analysis and Design of Space Vehicle Flight Control Systems, Volume VII – Attitude Control during Launch," *NASA* CR-826,1967
[5] Garner D, "Control theory Handbook", *NASA TM-X-53036*, 1964
[6] Astrom K. J., "Theory and Applications of Adaptive Control - A Survey", *Automatica 19(5)*, pages 471–486, 1983
[7] Boskovich B., and R. E. Kaufmann, "Evolution of the Honeywell First-Generation Adaptive Autopilot and Its Applications to F-94, F-101, X-15, and X-20 Vehicles", *AIAA Journal of Aircraft*, Volume 3, No. 4, pages 296-304, 1966
[8] Staff of the Flight Research Center, "Experience with the X-15 adaptive flight control system," *technical report, NASA Flight Research Center*, TN D-6208, 1971
[9] M. Thompson and J. Welsh, "Flight Test Experience With Adaptive Control Systems", *technical report, NASA Flight Research Center*, 1970.
[10] Landau. I. D., "A Survey of Model Reference Adaptive Techniques: Theory and Applications", *Automatica 10*, pages 353–379, 1974
[11] Kreisemayer. G., and B. Anderson, " Robust Model Reference Adaptive Control," *IEEE transactions on Automatic Control* AC-31(2), pages 127-133, 1986
[12] A. Khoshnood, J. Roshanian and A. Khaki-Sedig , "Model Reference Adaptive Control for a Flexible Launch Vehicle", Proc. IMechE Part I: Journal of Systems and Control Engineering,Vol.222 , pp.49-55, 2008.
[13] D.J. Leith and W.E.Leithead, "Survey of gain-scheduling analysis and design", International Journal of Control, Vol.73, No.11, 1001-1025, July 2000
[14] Jeb. S Orr., Tannen. S.VanZwieten, "Robust, Practical, Adaptive Control for Launch Vehicles", *AIAA Guidance, Navigation, and Control Conference* Minneapolis, Minnesota August 13-16, 2012.

APPENDIX

Notations used

A = reference area; D = drag

C_n =normal force coefficient

International Journal of Engineering Research & Technology (IJERT)
ISSN: 2278-0181
Vol. 5 Issue 04, April-2016

$\sum F_z$ = total force acting parallel to vehicle body axis, Z

I_{yy} = moment of inertia of reduced about pitch axis

I_0 = moment of inertia of rocket engine about its c.g.

I_r = moment of inertia of rocket engine about swivel point

K_A = servo amplifier gain

K_I = integrator gain

K_R = rate gyro gain;

V_w = wind velocity parallel to Z ' axis

l_C = distance from origin of body axis to engine swivel point

l_r = distance from c.g. of rocket to engine swivel point

l_α =distance from c.p. in pitch plane to origin of body axis

l_{pi} =distance from hinge point of ith pendulum to axis origin

L =length of vehicle

L_{pi} =length of ith pendulum

L_α =aerodynamic toad per unit angle of attack

$m(l)$ = reduced mass/length along vehicle longitudinal axis

m_0 = reduced mass of vehicle

m_{pi} = mass of ith pendulum

m_T = total mass of vehicle

m_R = mass of rocket engine

$M^{(i)}$ = generalized mass of ith bending mode

$\sum M_X$ = total perturbation moment about pitch axis

$q^{(i)}$ = generalized coordinate of ith bending mode

$Q^{(i)}$ = generalized force (moment) of ith bending mode

T_c =control thrust

T_s = ungimballed thrust

T_T =total thrust

$V = U_0$ = forward velocity of vehicle

$\dot{U}_0$ =acceleration

$\dot{z}$ = perturbation velocity of vehicle parallel to Z axis

α = perturbation angle of attack

γ = flight path angle

τ_{pi} = pendulum angle

δ = rocket engine deflection angle

δ_c = command signal to rocket engine

δ_N = nozzle deflection angle

δ_A = actuator deflection angle

ζ_a , ζ_N = relative damping factor for actuator, nozzle

$\zeta^{(i)}$ = relative damping ratio for ith bending mode

θ = perturbation attitude angle

θ_c= attitude command signal

$\xi(l,t)$ =bending deflection

$\sigma^{(i)}$ =slope of ith bending mode

$\psi^{(i)}$ = normalized mode function for the ith bending mode

ω_a , ω_N = undamped natural frequency for actuator, nozzle

ω_i , ω_{pi} =frequency of the ith bending mode, pendulum